NEOPLASIA
www.neoplasia.com

Volume 14 Number 4 April 2012 pp. 324–334 **324**

Quantitative Immunohistochemistry for Evaluating the Distribution of Ki67 and Other Biomarkers in Tumor Sections and Use of the Method to Study Repopulation in Xenografts after Treatment with Paclitaxel[1,2]

Andrea S. Fung*, James Jonkman† and Ian F. Tannock‡

*Department of Medical Biophysics, University of Toronto, Toronto, ON, Canada; †Advanced Optical Microscopy Facility, University Health Network, Toronto, ON, Canada; ‡Division of Medical Oncology and Hematology, Princess Margaret Hospital, Toronto, ON, Canada

Abstract

BACKGROUND: Surviving cells may repopulate tumors between courses of chemotherapy, thereby reducing the effectiveness of treatment. Using a novel quantitative method, we characterize the influence of the tumor microenvironment on repopulation of surviving cells in human tumor xenografts after paclitaxel treatment and evaluate the potential of gefitinib, an epidermal growth factor receptor (EGFR) inhibitor, to inhibit repopulation. *METHODS:* High-EGFR-expressing A431 xenografts and low-EGFR-expressing MCF-7 xenografts were treated with paclitaxel or gefitinib. Time-dependent changes in cell proliferation (Ki67) and apoptosis (cleaved caspase 3) in relation to total and functional tumor blood vessels (recognized by CD31 and a flow marker), and regions of hypoxia (recognized by EF5) were quantified using fluorescence microscopy. *RESULTS:* Decrease in functional tumor vasculature and in cell proliferation and increase in apoptosis were observed in A431 xenografts after treatment with either paclitaxel or gefitinib. There was a rebound in functional vasculature and cell proliferation ~12 days after treatment with paclitaxel, and repopulation was observed from tumor cells close to regions of hypoxia. Cell proliferation increased ~5 days after the last dose of gefitinib. There were minimal effects of paclitaxel or gefitinib on cell proliferation, cell death, or tumor vasculature in MCF-7 xenografts. *CONCLUSIONS:* Repopulation in A431 xenografts after treatment with paclitaxel was associated with changes in functional tumor vasculature. Gefitinib decreased cell proliferation in EGFR-overexpressing tumor xenografts, suggesting its potential to inhibit repopulation when used in sequence with chemotherapy.

Neoplasia (2012) 14, 324–334

Introduction

Limited studies have shown that surviving cells can repopulate a tumor between courses of chemotherapy [1–3], but little is known about the microenvironment in which cells repopulate within a solid tumor. The tumor microenvironment is composed of components that influence cell growth and cell death, including the tumor vasculature and regions of hypoxia. These factors allow for differing gradients in oxygenation, nutrients and pH, which influence the proliferation of cells within the tumor. In untreated tumors, cells proximal to functional blood vessels have a higher rate of proliferation than more distal tumor cells, most likely owing to better availability of nutrients and oxygen close to functional vasculature [2–5]. Many chemotherapeutic agents target selectively cells that are rapidly proliferating, and most drugs achieve a higher concentration close to blood vessels [4]; therefore, cells closer to blood vessels are more likely to be killed after chemotherapy.

Regions further from blood vessels contain viable tumor cells that may be spared by chemotherapy; these cells might repopulate the

Address all correspondence to: Ian F. Tannock, MD, PhD, Princess Margaret Hospital, Suite 5-208, 610 University Ave, Toronto, Ontario, Canada M5G 2M9. E-mail: ian.tannock@uhn.ca

[1]Supported by a grant from the Canadian Institutes of Health Research (MOP 15388). The authors have no conflicts of interest to declare.
[2]This article refers to supplementary material, which is designated by Figure W1 and is available online at www.neoplasia.com.
Received 14 February 2012; Revised 20 March 2012; Accepted 21 March 2012

DOI 10.1593/neo.12346

tumor if their nutrition improves after death and removal of more proximal cells. We hypothesize that repopulation will occur predominantly from regions of solid tumors distal from the vasculature after chemotherapy. In support of this hypothesis, Huxham et al. [2] showed that tumor cells in human colon cancer xenografts began proliferating in regions distal to blood vessels approximately 6 days after treatment with gemcitabine. However, repopulation has not been studied in other xenografts or human tumors or after treatment with different chemotherapeutic agents, including those that affect the tumor vasculature.

Many microenvironmental factors can influence the repopulation of tumor cells within a solid tumor. Changes in tumor vasculature can modify nutrient and oxygen gradients, thereby affecting the distribution of proliferating cells and dying cells within the tumor. Targeting the tumor vasculature can have both beneficial and detrimental effects—decreasing the tumor vasculature can limit the supply of nutrients and oxygen to tumor cells thereby leading to antitumor effects; however, decreased vasculature can also limit access of tumor cells to anticancer agents administered through the bloodstream [6–8]. Hypoxia also has a paradoxical effect on tumor growth. Prolonged or sustained hypoxia can result in cell death [9,10]; however, some tumor cells exposed to hypoxia might also acquire mutations that could lead to a more aggressive phenotype [10]. Because many anticancer agents have effects on the tumor microenvironment, it is imperative to understand how these factors contribute to repopulation within solid tumors.

Here we describe a novel method to quantify immunohistochemical staining in tumor sections to characterize changes in the distribution of repopulation within solid tumors. Our protocol differs from other methods in that it quantifies changes in immunohistochemical staining in the *whole* tumor section, rather than selecting areas of interest within a tumor; and it allows us to quantify cell proliferation and cell death as binary measurements. Therefore, we are able to reduce selection bias and account for heterogeneity in the tumor microenvironment. Specifically, the present study aims to: 1) characterize repopulation in A431 xenografts, a human squamous cell carcinoma that overexpresses the epidermal growth factor receptor (EGFR), and in low-EGFR-expressing MCF-7 xenografts, after treatment with paclitaxel; 2) determine the potential of gefitinib to inhibit repopulation; and 3) characterize changes in functional tumor vasculature and tumor hypoxia after treatment with chemotherapy. Our hypotheses are that repopulation will take place largely from poorly nourished cells distal from functional vasculature and that gefitinib will inhibit specifically repopulation in EGFR-overexpressing xenografts.

Materials and Methods

Cell Lines

Experiments were performed using the human vulvar epidermoid carcinoma cell line A431 (reported to overexpress EGFR) and the human breast carcinoma cell line MCF-7 (reported not to overexpress EGFR) [11]. A431 cells were purchased from the American Type Culture Collection (Manassas, VA). A431 cells were maintained in Dulbecco modified Eagle medium supplemented with 10% fetal bovine serum (HyClone, Logan, UT), and MCF-7 cells were grown in α-minimum essential medium with 10% fetal bovine serum. Cells were grown in a humidified atmosphere of 95% air/5% CO_2 at 37°C. Routine tests to exclude mycoplasma were performed. Expression of EGFR was confirmed by immunohistochemistry (Figure W1) using the mouse anti–human EGFR (Clone 31G7) antibody (Zymed Laboratories, San Francisco, CA).

Drugs and Reagents

Gefitinib (Iressa) was provided by AstraZeneca (Macclesfield, Cheshire, United Kingdom). Gefitinib was dissolved in 100% dimethyl sulfoxide (Fisher Scientific, Pittsburgh, PA) to make a 1-mg/ml stock solution, which was stored at 4°C; for *in vivo* studies, the stock solution was diluted in phosphate-buffered saline and 10% Solutol HS 15 (BASF Chemical Co, Ludwigshafen, Germany). Paclitaxel was purchased from the hospital pharmacy as a 6-mg/ml stock solution and stored at room temperature. EF5 was provided by the National Cancer Institute, and Cy5-conjugated mouse anti-EF5 antibody was purchased from Dr. Cameron Koch, University of Pennsylvania, PA. EF5 powder was dissolved in distilled water and 2.4% ethanol and 5% dextrose to make a 10-mM stock solution that was stored at room temperature. DiOC7 was purchased from AnaSpec Inc. (San Jose, CA) and a stock solution (2.5 mg/ml) was made by dissolving in dimethyl sulfoxide. The stock was diluted 1:10 in phosphate-buffered saline and 10% Solutol HS 15.

Effect of Paclitaxel and Gefitinib on Growth of Xenografts

Female athymic nude mice (4-6 weeks old) (Harlan Sprague-Dawley, Madison, WI) were injected subcutaneously in both flanks with 1×10^6 A431 cells or 4×10^6 MCF-7 cells per side; before injection of MCF-7 cells, mice were implanted with 17β-estradiol tablets (60-day release; Innovative Research of America, Sarasota, FL). There were five mice per treatment group (10 tumors), and each experiment was repeated. Two perpendicular diameters were measured with a caliper, and once tumors reached a diameter of 5 to 8 mm, treatment commenced. Tumor volume was estimated using the formula: $0.5(ab^2)$, where a and b are the longer and shorter diameters, respectively.

To determine effects of paclitaxel, mice were treated intraperitoneally (i.p.) once every 5 days for a total of three doses of 0, 10, 20, or 30 mg/kg body weight. To test the effects of gefitinib alone, doses of 50 or 100 mg/kg were administered by oral gavage daily for 3 d/wk for 2 weeks. Tumor size and body weight were measured every other day until tumors grew to a maximum diameter of 1.5 cm or caused ulceration, when mice were killed humanely. To avoid bias, mice were ear tagged and randomized, and measurements were made without knowledge of the treatment history.

Effect of Paclitaxel and Gefitinib on Cell Proliferation and Apoptosis

Mice with tumors of 5 to 8 mm in diameter were treated with paclitaxel alone (a single 25-mg/kg dose administered i.p. on day 0) or gefitinib alone (a dose of 100 mg/kg administered by oral gavage daily for 3 days). Mice were killed humanely, and tumors were excised on days 0, 2, 4, 6, 8, 10, and 12. There were three to five mice per time point in both the paclitaxel or gefitinib treatment groups. The hypoxia-selective agent EF5 (0.2 ml of 10 mM stock solution) was injected i.p. ~2 hours before killing the mice, and the perfusion marker DiOC7 (1 mg/kg) was injected intravenously 1 minute before killing the mice. Tumors were excised, immersed in OCT compound, and frozen in liquid nitrogen. Tumors were cut into 10-μm-thick sections and imaged using an Olympus BX50 fluorescence (Olympus, Center Valley, PA) and bright-field microscope equipped for whole-slide imaging using tiling and stitching.

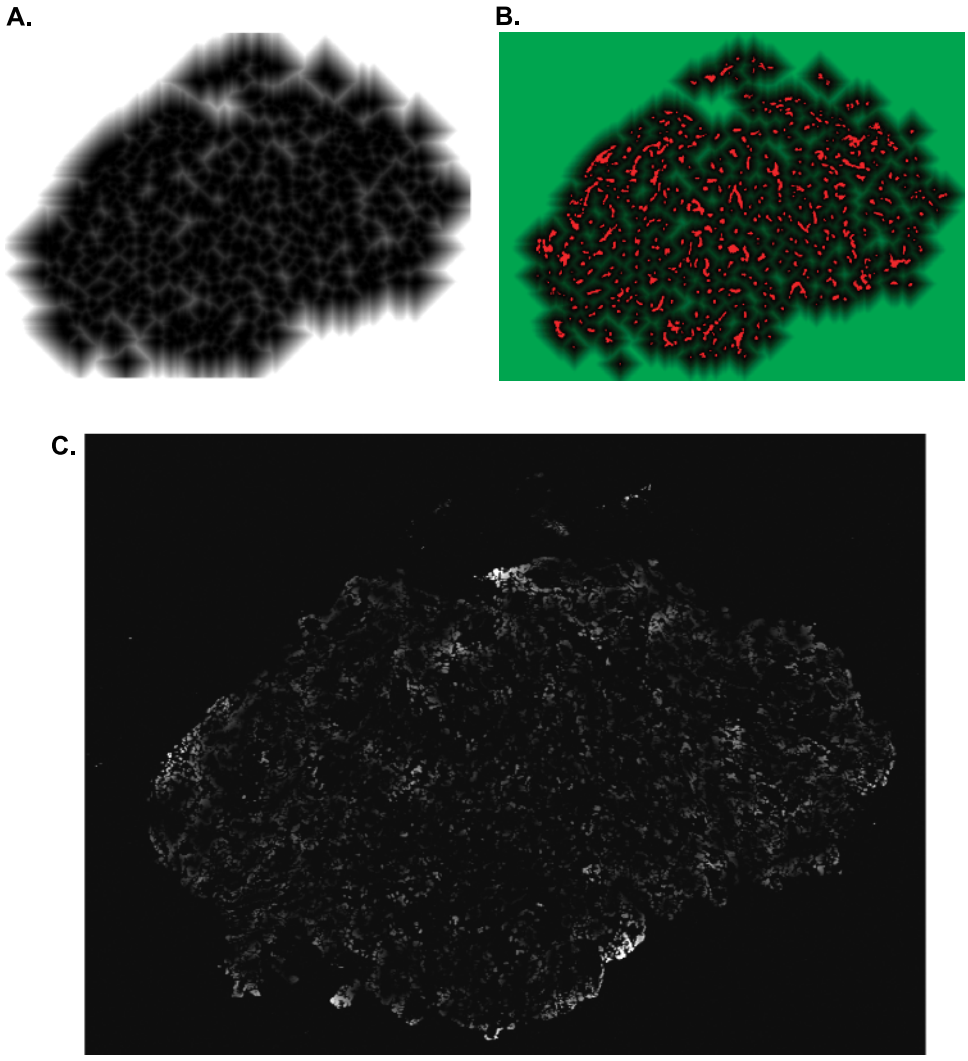

Figure 1. (A) Grayscale image showing gradient of pixel distances in relation to the nearest functional blood vessel (white = farthest distance from blood vessel, black = location of blood vessel). (B) Color composite of the gradient of pixel distances shown in panel A (pseudocolored green) and the blood vessel marker (binarized and pseudocolored red). (C) Distance image of a tumor section showing gradient of distance units corresponding to all Ki67/cleaved caspase 3–positive pixels (grayscale image: white represents farthest distance from blood vessel and black represents a distance unit of zero)—similar methods were used for quantifying cleaved caspase 3.

Tumor sections were first imaged for the perfusion marker DiOC7 using an fluorescein isothiocyanate filter set. Sections were then stained for blood vessels using a rat anti-CD31 primary antibody (BD Biosciences, Toronto, Canada) and Cy3-conjugated goat anti-rat IgG secondary antibody. Hypoxic regions were identified using a Cy5-conjugated mouse anti-EF5 antibody, proliferating cells were stained for Ki67 (rabbit anti–human Ki67 antibody, HRP chromogen; Novus, Oakville, Canada), and apoptotic cells were stained for cleaved caspase 3 (rabbit anti–human cleaved caspase 3 antibody, HRP chromogen; Cell Signaling, Danvers, MA). Tumor sections were imaged for CD31 using the Cy3 filter set, and EF5 was imaged using the Cy5 far-red filter set. Ki67 and cleaved caspase 3 were imaged using transmitted light.

Image Analysis and Quantification

Microscope images of tumor vasculature and hypoxia were quantified using Media Cybernetics Image Pro PLUS software (Bethesda, MD). A threshold was used to select pixels occupied by blood vessels, as represented by CD31 staining, and the image was binarized by setting these blood vessel regions to white (pixel value, 255) and background pixels to black (pixel value, 0) to form a "mask" of positive CD31 staining. Using Image Pro's Count/Size tool, objects with a pixel intensity of 255 (i.e., CD31-positive) were counted in each tumor section. The tumor area (excluding areas of necrosis or artifacts) was measured using Image Pro's calibrated area measurement tool. The mean number of total blood vessels per tumor area was calculated. A similar method was used to evaluate functional blood vessels: the total number of objects in DiOC7 binarized images was counted and the number of DiOC7-positive objects was divided by the number of CD31-positive objects to provide an estimate of the proportion of functional vessels in each tumor section. Total vasculature includes all blood vessels stained by CD31, whereas functional tumor vasculature includes only those vessels that have functional blood flow (as measured by the perfusion marker DiOC7).

Hypoxia was evaluated by setting a threshold on the EF5 image and using Image Pro's Count/Size tool to determine the total area of pixels selected by the threshold. The percentage of hypoxia was

calculated by taking the area of EF5-positive staining and dividing it by the total tumor area. We did not attempt to differentiate the level of hypoxia, as reflected by intensity of EF5 staining.

A novel protocol was developed, based on the method described by Primeau et al. [4], which analyzes Ki67 (proliferation) and cleaved caspase 3 (apoptosis) images to measure the location of these markers relative to blood vessels. The binarized DiOC7 fluorescence image was used as the input to Image Pro's Distance Map filter creating a new image where each pixel's intensity represents its distance to the nearest functional blood vessel in the section (Figure 1, *A* and *B*). To evaluate distributions of cell proliferation and apoptosis relative to functional blood vessels, Ki67 and cleaved caspase 3 bright-field images were thresholded for positive staining and binarized images (masks) were created. The Ki67 or cleaved caspase 3 mask was combined with the distance map using a pixel-by-pixel logical "AND" function, thereby creating a unique image where black regions (zero intensity) contain no Ki67, and nonzero regions are positive for Ki67 with the intensity values representing the distance to the nearest blood vessel rather than the usual staining intensity (Figure 1*C*).

Because solid tumors are three-dimensional, blood vessels out of the plane of the tissue sections might confound the above analysis, especially for quantification of cellular properties in regions distal to blood vessels in a section. Therefore, Ki67 staining was also evaluated in relation to the nearest hypoxic region (identified by EF5) to obtain a more accurate distribution of cell proliferation in regions distal from functional blood vessels. The EF5 fluorescence image was converted to a black and white binarized image (mask), which was used to generate a map of distances between pixels and regions of hypoxia. The distance map was combined with the corresponding Ki67 mask to determine the mean frequency of Ki67-positive pixels at distances from the nearest region of hypoxia.

Data are represented graphically as the mean frequency of Ki67/cleaved caspase 3–positive pixels (normalized for area) at each distance (0-100 μm) from the nearest blood vessel or region of hypoxia.

Statistical Analysis

For total and functional tumor vasculature and hypoxia, *t* tests were performed to determine the significance of differences between groups. Linear regression was used to evaluate the distributions of cell proliferation and apoptosis, as a function of distance to the nearest blood vessel (or hypoxic region). The slopes and Y-intercepts (i.e., the perivascular levels) were calculated and compared for all tumor samples. Differences in the slope and Y-intercepts indicated changes in the spatial distribution of the measured marker (e.g., Ki67 for cell proliferation) in relation to functional blood vessels. A one-way ANOVA, followed by Tukey *post hoc* test, determined statistical

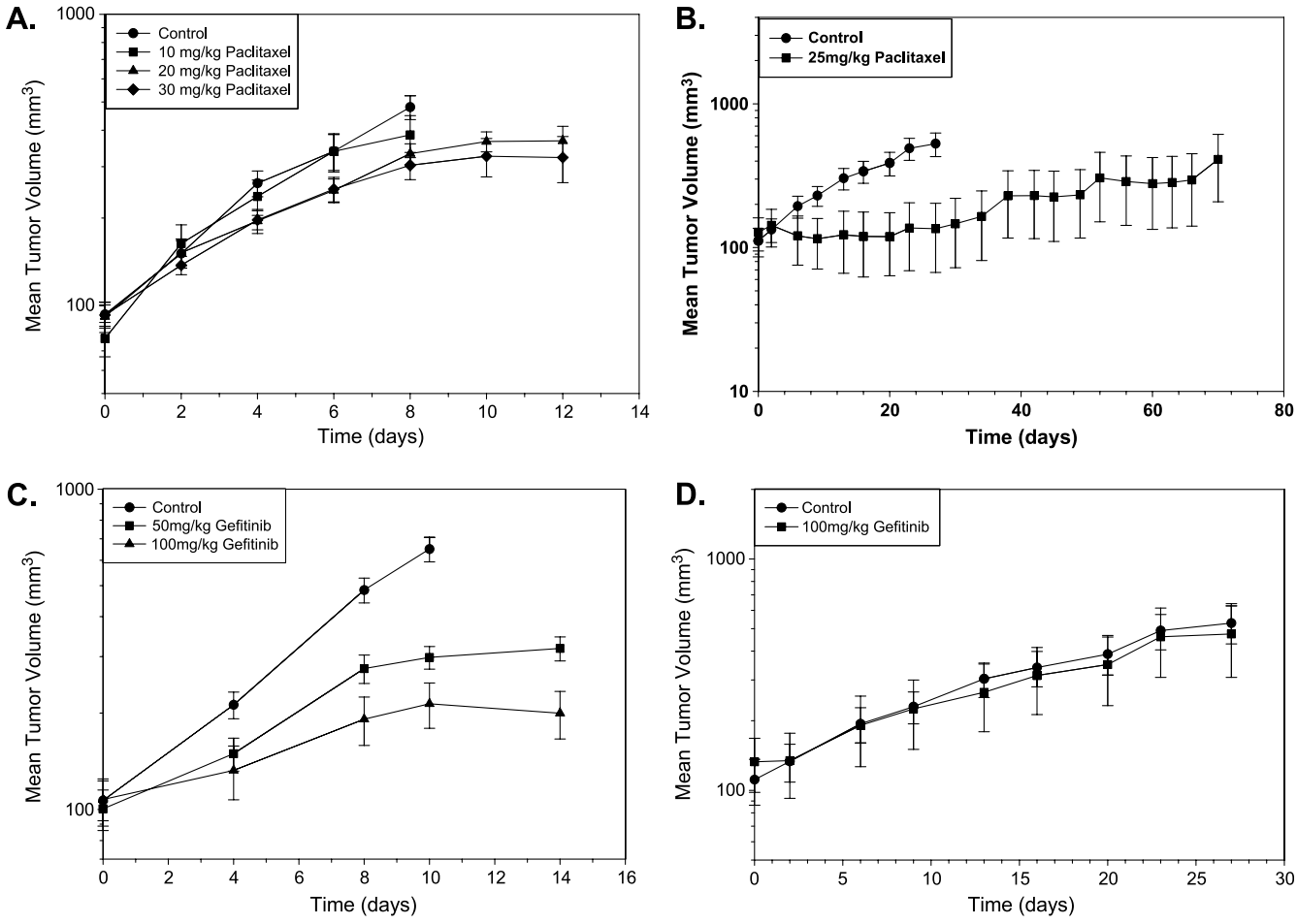

Figure 2. The effect of paclitaxel (10-30 mg/kg i.p. once every 5 days for three total doses) on (A) growth of A431 xenografts in nude mice and (B) growth of MCF-7 xenografts in nude mice (points indicate mean for 5 mice per group; bars, SE). The effect of gefitinib (50 or 100 mg/kg by oral gavage, 3 d/wk for 2 weeks) on the growth of (C) A431 (points indicate mean of two independent experiments, 10 mice per group; bars, SE) or (D) MCF-7 (points indicate mean of 5 mice per group; bars, SE) xenografts in nude mice.

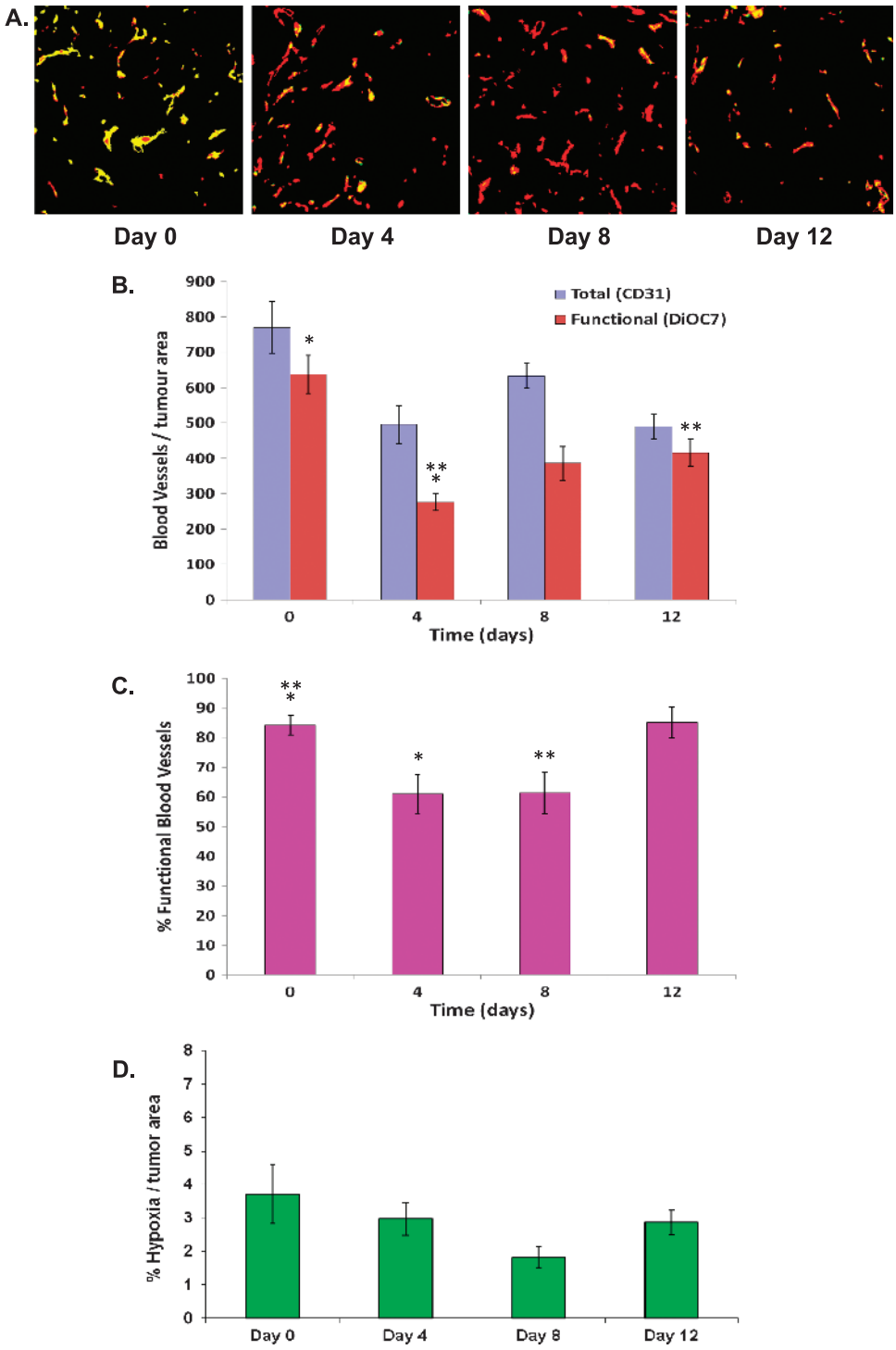

Figure 3. (A) Photomicrographs of tumor blood vessels after a single dose of paclitaxel (25 mg/kg, i.p.) in A431 xenografts (red = CD31 [total vessels], yellow = DiOC7 [functional vessels]); day 0 = untreated tumors. (B) The number of total and functional blood vessels. (C) The percentage of functional tumor vasculature. (D) The percentage of hypoxia. *Statistical significance ($P < .05$) between groups.

differences between treatment groups. $P < .05$ was used to indicate statistical significance; all tests were two sided.

Results

Effects of Paclitaxel and Gefitinib on Growth of Xenografts

There were dose-dependent effects of paclitaxel on A431 tumor growth with no significant loss of body weight of the mice for the range of doses evaluated (Figure 2*A*). MCF-7 xenografts grew more slowly than A431 xenografts, and paclitaxel caused greater delay in their growth (Figure 2*B*).

Gefitinib inhibited growth of A431 (EGFR+++) xenografts in a dose-dependent manner (Figure 2*C*), but there was rapid regrowth of the tumor once gefitinib treatment was stopped (data not shown). As expected, there was no effect of gefitinib to inhibit the growth of low EGFR-expressing MCF-7 xenografts compared with control tumors (Figure 2*D*).

Changes in Vasculature and Hypoxia after Treatment of Xenografts with Paclitaxel or Gefitinib

The concentration of blood vessels (as measured by CD31 staining) per tumor area decreased after paclitaxel treatment and was significantly lower in A431 tumors on days 4 and 12 compared with untreated tumors (Figure 3, *A* and *B*; $P = .007$ and $P = .004$, respectively). There was a significant decrease in the number of functional blood vessels per tumor area measured 4 days after paclitaxel (Figure 3*B*; $P = .0001$) followed by a rebound on days 8 and 12 (Figure 3*B*; day 4 *vs* day 12, $P = .01$), although the number of functional vessels remained lower than in untreated tumors. The percentage of functional blood vessels in A431 xenografts on days 4 and 8 after paclitaxel treatment was lower than in untreated tumors (Figure 3, *A* and *C*; $P = .006$ and $P = .008$, respectively), followed by a rebound at 12 days. There was a trend to decreased hypoxia (per

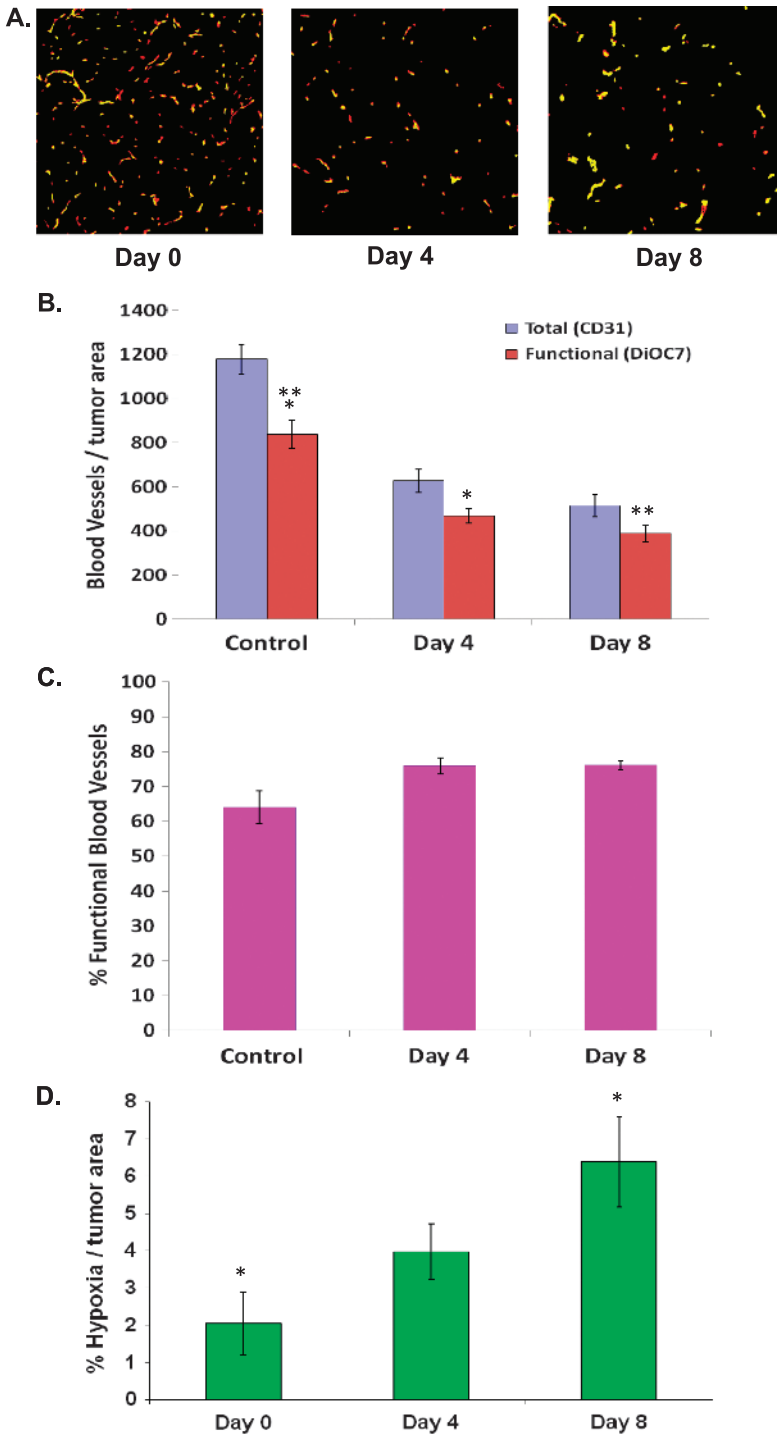

Figure 4. (A) Photomicrographs of tumor blood vessels in A431 xenografts treated with gefitinib (100 mg/kg, days 0-3; red = CD31, yellow = DiOC7). (B) The number of total and functional blood vessels. (C) The percentage of functional tumor vasculature. (D) The percentage of hypoxia. *Statistical significance ($P < .05$) between groups.

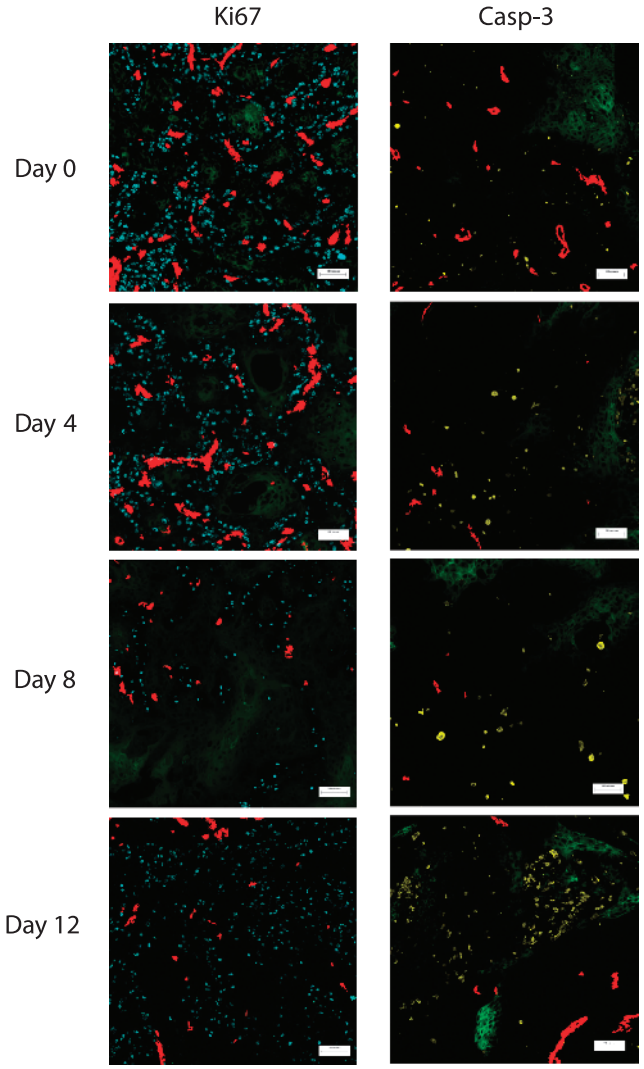

Figure 5. The distribution of proliferating (blue, left panel) or apoptotic cells (yellow, right panel) in relation to functional blood vessels (red) and regions of hypoxia (green) in A431 xenografts on days 0 (untreated), 4, 8, and 12 after paclitaxel treatment. Scale bars, 100 μm.

tumor area) in tumors taken on day 8 when compared with untreated controls ($P = .07$) followed by a rebound on day 12 (Figure 3*D*).

Three days of gefitinib treatment caused a decrease in the total number of blood vessels (i.e., CD31-positive vessels; $P < .05$) and in the total number of functional blood vessels per tumor area in A431 tumors on days 4 and 8 compared with untreated tumors ($P < .05$; Figure 4, *A* and *B*). However, there was no significant change in the percentage of functional vessels compared with untreated tumors (Figure 4, *A* and *C*; $P > .05$). There was an increase in the percentage of hypoxia on day 8 (i.e., 5 days after the last dose of gefitinib) compared with untreated controls (Figure 4*D*; $P = .01$), likely related to the observed decrease in perfused vessels.

Treatment of MCF-7 xenografts with either paclitaxel or gefitinib led to no significant changes in total blood vessels or in the percentage of functional vasculature. There was a transient increase in hypoxia in MCF-7 xenografts on day 3 after paclitaxel or gefitinib treatment compared with untreated tumors (data not shown).

Effect of Paclitaxel on the Distribution of Cell Proliferation and Apoptosis in Xenografts

There was a high intensity of Ki67 staining in untreated A431 xenografts, and cell proliferation decreased with increasing distance from the nearest functional blood vessel (Figures 5 and 6*A*). The maximum Ki67 staining at ~20 μm from the nearest blood vessel likely represents perivascular tumor cells.

At 4 and 8 days after a single 25-mg/kg dose of paclitaxel, there was a decrease in cell proliferation in regions close to blood vessels and in intermediate regions (Figure 6*A*; $P < .05$). On day 12 after paclitaxel treatment, there was a rebound in Ki67 staining (Figure 6*A*; day 8 *vs* day 12, $P < .05$). There was a low level of Ki67 staining near hypoxic regions in untreated tumors, and cell proliferation increased with greater distance from hypoxic regions (Figure 6*B*). Cell proliferation remained low near hypoxic regions on days 4 and 8 after paclitaxel treatment, but by day 12, there was a substantial increase in the proliferation of cells near hypoxic regions, indicating repopulation from these formerly quiescent cells (Figure 6*B*; $P < .05$).

There were few apoptotic cells in untreated A431 tumors with minimal dependence on distance from functional blood vessels (Figures 5 and 6*C*). There was an increase in apoptotic cells staining for cleaved caspase 3 in regions proximal and distal from functional blood vessels on day 12 after paclitaxel treatment when compared with untreated tumors (Figure 6*C*). An increase in the necrotic fraction was also noted in day 8 and day 12 tumors compared with untreated controls.

Analysis of MCF-7 tumor sections showed a relatively uniform distribution of cell proliferation and cell death (as measured by the necrotic fraction because MCF-7 cells do not express caspase 3) in untreated tumors with no significant change in these distributions after a single 25-mg/kg dose of paclitaxel (data not shown).

Effect of Gefitinib on the Distribution of Cell Proliferation and Apoptosis in Xenografts

On day 4 (i.e., 1 day after the end of 3 days of gefitinib treatment), there was a significant decrease in the level of Ki67 staining in regions proximal to functional blood vessels followed by a rebound in tumor samples taken on day 8 (Figure 7*A*; $P < .01$ for day 0 *vs* day 4 and for day 4 *vs* day 8). There was an increase in apoptosis in A431 tumors on days 4 and 8 when compared with untreated tumors and the level of cleaved caspase 3 staining was higher in regions more distal to functional blood vessels after gefitinib treatment (Figure 7*B*; $P < .05$).

In MCF-7 tumors, there was an increase in cell proliferation near blood vessels on day 3 of gefitinib treatments, but by day 5, cell proliferation decreased to levels similar to untreated controls. There was no change in the distribution of cell death after gefitinib treatment (data not shown).

Discussion

Repopulation of surviving tumor cells after chemotherapy is likely to be influenced by many factors within the tumor microenvironment, including the distribution of drug within the tumor tissue, and changes in tumor vasculature and hypoxia. Here we show that, after treatment of A431 xenografts with paclitaxel, there was an initial decrease in the percentage of functional blood vessels followed by a partial recovery (Figure 3*C*). Similarly, there was a decrease in cell proliferation in tumor regions close to blood vessels, but proliferation increased at 12 days after treatment and was observed in regions

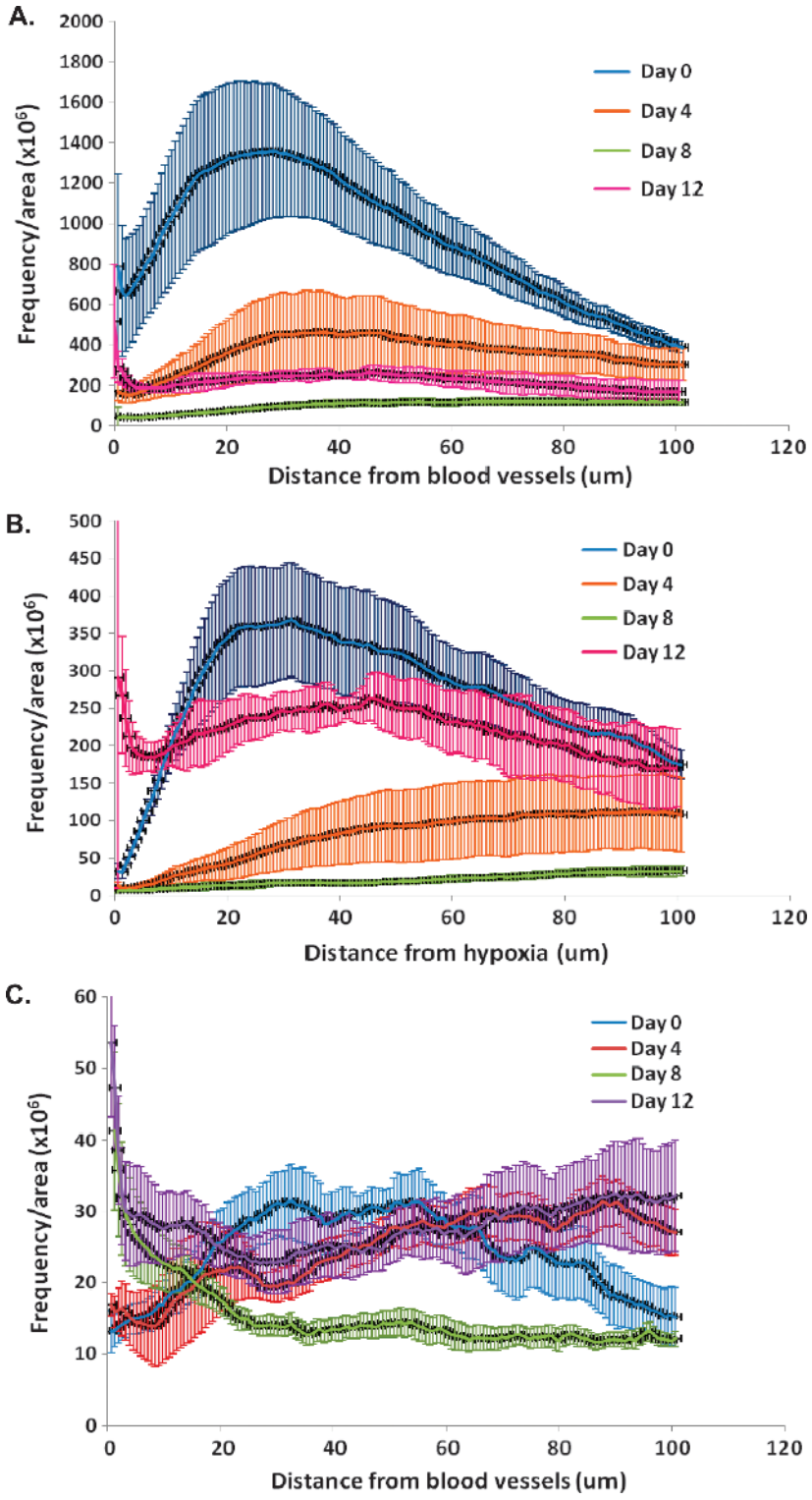

Figure 6. The effect of a single dose of paclitaxel (25 mg/kg) on cell proliferation in A431 xenografts, as measured by Ki67 staining in relation to distance from the nearest (A) functional blood vessel and (B) hypoxic region. (C) Effect of paclitaxel on apoptosis, as measured by cleaved caspase 3 staining, in relation to distance from the nearest functional blood vessel. Lines indicate the mean of four to six tumors per treatment group; error bars, SE.

both proximal to blood vessels and among cells in and adjacent to hypoxic regions (Figure 6, *A* and *B*). The effect of paclitaxel on cell proliferation could be two-fold: 1) an initial decrease in cell proliferation in regions proximal to blood vessels due to cytotoxic and cytostatic effects of paclitaxel, which is likely well distributed to proximal regions; and 2) effects of paclitaxel to decrease functional vasculature. With less functional vasculature, there is likely a subsequent decrease in oxygen and nutrients available to cells within the tumor, which could lead to inhibition of cell proliferation and to cell death [10,12–14].

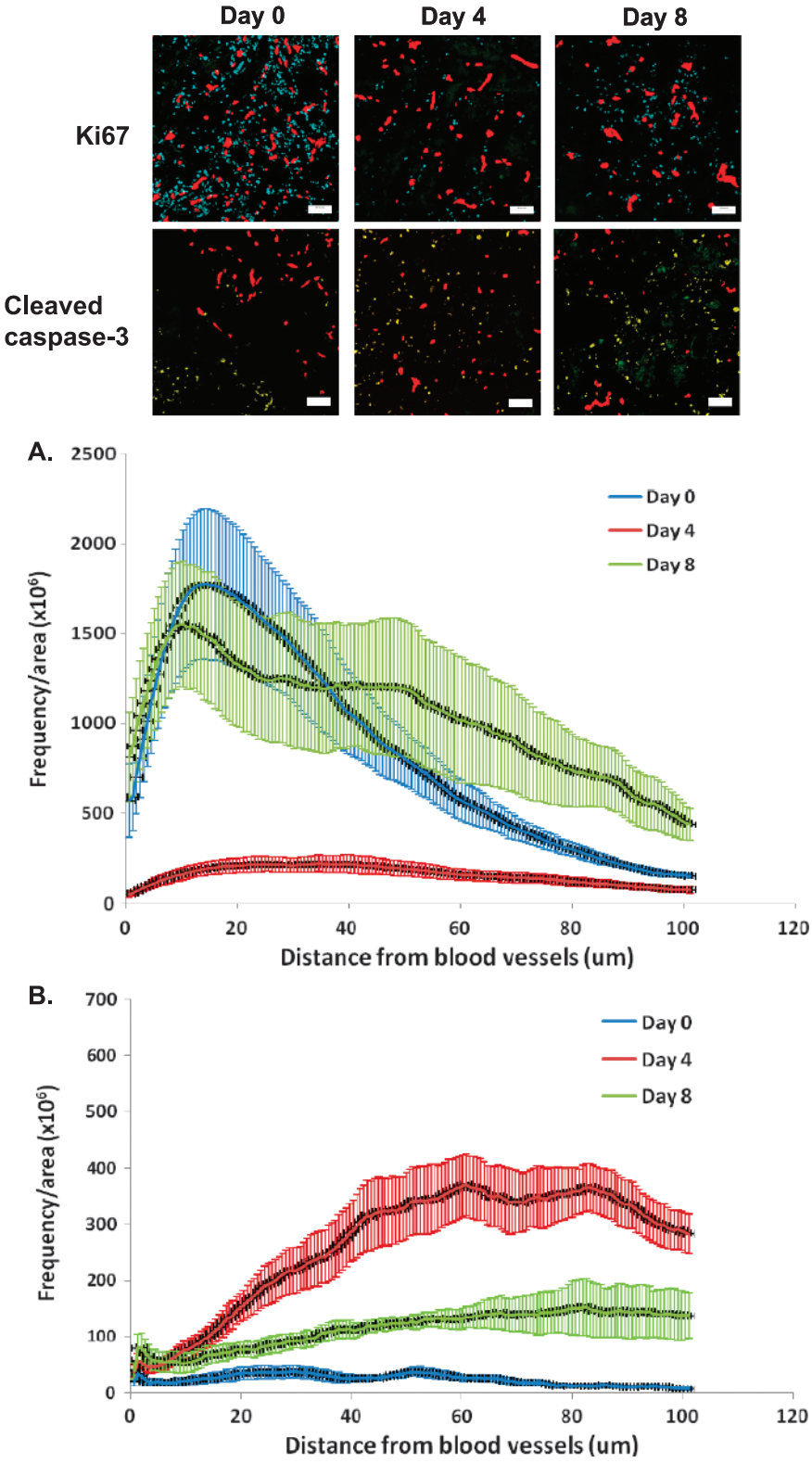

Figure 7. The effect of gefitinib (100 mg/kg by oral gavage, 3 days of treatment) on (A) cell proliferation (Ki67) and (B) apoptosis (cleaved caspase 3) in A431 xenografts. Time is measured from the start of the gefitinib treatments (i.e., day 4 is 1 day after the last treatment). Photomicrographs: blue = Ki67, yellow = cleaved caspase 3, and red = functional blood vessels. Plots indicate the frequency of positively stained pixels in relation to distance from the nearest functional blood vessel. Lines indicate the mean of four to six tumors per treatment group; error bars, SE.

Despite the importance of repopulation in the design of optimal chemotherapy for solid tumors, we are aware of only one prior study that has shown that the process may originate largely from regions distal from functional vasculature, in essence rescuing tumor cells that would have died in the absence of treatment; this is in stark contrast to the study of repopulation after radiotherapy where repopulation from surviving hypoxic tumor cells is well established. Huxham et al. [2] described the distribution of repopulation in human colorectal carcinoma xenografts after treatment with gemcitabine. They showed that repopulation commenced in regions further from blood vessels approximately 6 days after gemcitabine treatment [2]. Studies by Shaked et al. [15] showed that some drugs, including paclitaxel, decrease microvascular density, whereas others, including gemcitabine, have little or no effect. Here we have characterized the effect of the widely used anticancer drug, paclitaxel, on the spatial distribution of repopulation in solid tumors. Our data suggest that the rebound in the percentage of functional tumor vessels in A431 xenografts approximately 12 days after paclitaxel treatment might be associated with a corresponding rebound in cell proliferation (Figures 3*C* and 6, *A* and *B*). Changes in functional blood vessels are more important than changes in total blood vessels, highlighting the importance of using perfusion markers in conjunction with CD31 staining; CD31 is expressed on endothelial cells but does not provide information on vessel function [16]. Improved availability of nutrients could stimulate repopulation of the tumor cells [17]. The rebound in proliferation of cells close to regions of hypoxia is particularly noteworthy on day 12 (Figure 6*B*), and this might be due to better access to nutrients and/or the proliferation of previously quiescent populations.

The observed discrepancy in hypoxic fractions after paclitaxel or gefitinib treatment (despite similar antivascular effects) could be due to the higher proportion of cell death noted after paclitaxel compared with gefitinib treatment; the increased cell loss might promote reoxygenation through decreased oxygen consumption (due to fewer surviving cells) and improved access of surviving cells to blood vessels after the removal of dead cells proximal to vessels [18].

The concentration of cells within solid tumors may affect vascular perfusion and might be modified after chemotherapy [17]. Griffon-Etienne et al. [17] showed an increase in blood vessel diameter and vascular flow (as measured by red blood cell velocity) at 2 to 4 days after paclitaxel treatment of human soft tissue sarcoma xenografts; this was likely due to an increase in cell death surrounding blood vessels leading to a reduction in the number of collapsed vessels. Likewise, Kuh et al. [19] observed apoptosis 24 hours after treatment, which corresponded to an observed increase in penetration of paclitaxel within the tumor. Our data show an increase in apoptosis and necrosis after paclitaxel treatment in A431 xenografts (Figure 6*C*). Changes in apoptosis seem to correlate with the rebound in proliferation after paclitaxel treatment, particularly in distal regions at later time points (i.e., day 12 tumors)—apoptosis observed in distal cells could be due to cytotoxic effects or inadequate nutrients before tumor excision, whereas simultaneous proliferation in distal regions could stem from a population of cells that did not undergo apoptosis because of resistance mechanisms or a previously quiescent state protecting the cell from cytotoxicity from paclitaxel treatment. Apoptosis probably contributes only to a small fraction of cell death after chemotherapy for solid tumors [20,21]; however, recent data suggest that apoptosis, and specifically activated caspase 3, may be associated with stimulation of repopulation after radiotherapy [22], and this may also occur after chemotherapy. This might explain the limited repopulation observed after treatment of caspase 3–deficient MCF-7 xenografts with paclitaxel.

In the present study, we have used a novel computer-based image analysis program to quantify cell proliferation and apoptosis in relation to blood vessels and hypoxia in tumor sections. This method overcomes some of the limitations associated with older methods including its ability to quantify cell proliferation (Ki67) and apoptosis (cleaved caspase 3) as binary measurements. Also we analyzed the whole tumor section rather than averaging results from multiple smaller areas of interest, thereby avoiding bias associated with selecting areas of interest (Figure 1).

Targeted agents might be used to inhibit repopulation in solid tumors between courses of chemotherapy. An ideal inhibitor is fast acting and has effects to inhibit tumor cell proliferation that are not prolonged once the inhibitor is removed, thus allowing cells to reenter cycle before the next course of cycle-active chemotherapy. Gefitinib inhibited proliferation of EGFR-overexpressing A431 xenografts in regions both proximal and distal to functional blood vessels (Figure 7*A*). Cell proliferation rebounded by day 8, approximately 5 days after the last dose of gefitinib was administered (Figure 7*A*). Gefitinib has antiangiogenic properties and can inhibit endothelial cell proliferation [23–25]. There were moderate effects of gefitinib to change the percentage of functional vessels (Figure 4*C*), which could account for the more rapid rebound in cell proliferation near perfused vessels after gefitinib compared with treatment with paclitaxel.

Clinically, EGFR inhibitors such as gefitinib and erlotinib have shown some effects to prolong survival or delay tumor progression when used alone [26–28], but have had minimal benefit when used concurrent with chemotherapy compared with chemotherapy alone [29–31]. It is possible that treatment scheduling played a role in the negative outcome of these clinical trials because cells might have been out of cycle because of inhibition of growth due to the EGFR inhibitor, thereby rendering them less susceptible to cycle-active chemotherapy. We report elsewhere that gefitinib administered sequentially between courses of paclitaxel can inhibit repopulation of A431 cells [32], but determining an optimal schedule *in vivo* is likely to be complex and should take into account effects on the microenvironment, including changes in the functional tumor vasculature and in hypoxia. It is likely that combining chemotherapeutic agents and targeted agents that affect tumor vasculature will result in antiproliferative, as well as antivascular effects, that can impact the occurrence and distribution of repopulation in solid tumors.

In summary, we have used a novel quantitative method to detect changes in the distribution of repopulation in solid tumors. We have shown that repopulation occurs in A431 xenografts after paclitaxel treatment and that proliferation of surviving cells occurs in regions both proximal and distal to functional blood vessels. Furthermore, our study highlights the interaction between repopulation and changes in functional blood vessels. Gefitinib has the potential to inhibit repopulation between courses of chemotherapy due to its ability to decrease cell proliferation during drug treatment while also allowing cells to reenter cycle soon after removal of the drug. Gefitinib administered sequentially between courses of paclitaxel might be effective in inhibiting repopulation of tumor cells.

Acknowledgments

The authors thank all members of the Pathology Research Program and the Advanced Optical Microscopy Facility.

References

[1] Wu L and Tannock IF (2003). Repopulation in murine breast tumors during and after sequential treatments with cyclophosphamide and 5-fluorouracil. *Cancer Res* **63**, 2134–2138.

[2] Huxham LA, Kyle AH, Baker JH, Nykilchuk LK, and Minchinton AI (2004). Microregional effects of gemcitabine in HCT-116 xenografts. *Cancer Res* **64**, 6537–6541.

[3] Kim JJ and Tannock IF (2005). Repopulation of cancer cells during therapy: an important cause of treatment failure. *Nat Rev Cancer* **5**, 516–525.

[4] Primeau AJ, Rendon A, Hedley D, Lilge L, and Tannock IF (2005). The distribution of the anticancer drug doxorubicin in relation to blood vessels in solid tumors. *Clin Cancer Res* **11**, 8782–8788.

[5] Tredan O, Galmarini CM, Patel K, and Tannock IF (2007). Drug resistance and the solid tumor microenvironment. *J Natl Cancer Inst* **99**, 1441–1454.

[6] Jang SH, Wientjes MG, Lu D, and Au JL (2003). Drug delivery and transport to solid tumors. *Pharm Res* **20**, 1337–1350.

[7] Folkman J (2006). Angiogenesis. *Annu Rev Med* **57**, 1–18.

[8] Fukumura D and Jain RK (2007). Tumor microenvironment abnormalities: causes, consequences, and strategies to normalize. *J Cell Biochem* **101**, 937–949.

[9] Hockel M and Vaupel P (2001). Tumor hypoxia: definitions and current clinical, biologic, and molecular aspects. *J Natl Cancer Inst* **93**, 266–276.

[10] Vaupel P and Mayer A (2007). Hypoxia in cancer: significance and impact on clinical outcome. *Cancer Metastasis Rev* **26**, 225–239.

[11] Rusnak DW, Alligood KJ, Mullin RJ, Spehar GM, Arenas-Elliott C, Martin AM, Degenhardt Y, Rudolph SK, Haws TF Jr, Hudson-Curtis BL, et al. (2007). Assessment of epidermal growth factor receptor (EGFR, ErbB1) and HER2 (ErbB2) protein expression levels and response to lapatinib (Tykerb, GW572016) in an expanded panel of human normal and tumour cell lines. *Cell Prolif* **40**, 580–594.

[12] Vaupel P, Kallinowski F, and Okunieff P (1989). Blood flow, oxygen and nutrient supply, and metabolic microenvironment of human tumors: a review. *Cancer Res* **49**, 6449–6465.

[13] Olive PL, Vikse C, and Trotter MJ (1992). Measurement of oxygen diffusion distance in tumor cubes using a fluorescent hypoxia probe. *Int J Radiat Oncol Biol Phys* **22**, 397–402.

[14] Dewhirst MW (1998). Concepts of oxygen transport at the microcirculatory level. *Semin Radiat Oncol* **8**, 143–150.

[15] Shaked Y, Henke E, Roodhart JM, Mancuso P, Langenberg MH, Colleoni M, Daenen LG, Man S, Xu P, Emmenegger U, et al. (2008). Rapid chemotherapy-induced acute endothelial progenitor cell mobilization: implications for antiangiogenic drugs as chemosensitizing agents. *Cancer Cell* **14**, 263–273.

[16] Scholz D and Schaper J (1997). Platelet/endothelial cell adhesion molecule-1 (PECAM-1) is localized over the entire plasma membrane of endothelial cells. *Cell Tissue Res* **290**, 623–631.

[17] Griffon-Etienne G, Boucher Y, Brekken C, Suit HD, and Jain RK (1999). Taxane-induced apoptosis decompresses blood vessels and lowers interstitial fluid pressure in solid tumors: clinical implications. *Cancer Res* **59**, 3776–3782.

[18] Milas L, Hunter NR, Mason KA, Milross CG, Saito Y, and Peters LJ (1995). Role of reoxygenation in induction of enhancement of tumor radioresponse by paclitaxel. *Cancer Res* **55**, 3564–3568.

[19] Kuh HJ, Jang SH, Wientjes MG, Weaver JR, and Au JL (1999). Determinants of paclitaxel penetration and accumulation in human solid tumor. *J Pharmacol Exp Ther* **290**, 871–880.

[20] Tannock IF and Lee C (2001). Evidence against apoptosis as a major mechanism for reproductive cell death following treatment of cell lines with anti-cancer drugs. *Br J Cancer* **84**(1), 100–105.

[21] Brown JM and Attardi LD (2005). The role of apoptosis in cancer development and treatment response. *Nat Rev Cancer* **5**, 231–237.

[22] Huang Q, Li F, Liu X, Li W, Shi W, Liu FF, O'Sullivan B, He Z, Peng Y, Tan AC, et al. (2011). Caspase 3–mediated stimulation of tumor cell repopulation during cancer radiotherapy. *Nat Med* **17**(7), 860–867.

[23] Hirata A, Uehara H, Izumi K, Naito S, Kuwano M, and Ono M (2004). Direct inhibition of EGF receptor activation in vascular endothelial cells by gefitinib ("Iressa," ZD1839). *Cancer Sci* **95**, 614–618.

[24] Amin DN, Hida K, Bielenberg DR, and Klagsbrun M (2006). Tumor endothelial cells express epidermal growth factor receptor (EGFR) but not ErbB3 and are responsive to EGF and to EGFR kinase inhibitors. *Cancer Res* **66**, 2173–2180.

[25] Amin DN, Bielenberg DR, Lifshits E, Heymach JV, and Klagsbrun M (2008). Targeting EGFR activity in blood vessels is sufficient to inhibit tumor growth and is accompanied by an increase in VEGFR-2 dependence in tumor endothelial cells. *Microvasc Res* **76**, 15–22.

[26] Kris MG, Natale RB, Herbst RS, Lynch TJ, Prager D, Belani CP, Schiller JH, Kelly K, Spiridonidis H, Sandler A, et al. (2003). Efficacy of gefitinib, an inhibitor of the epidermal growth factor receptor tyrosine kinase, in symptomatic patients with non–small cell lung cancer: a randomized trial. *JAMA* **290**, 2149–2158.

[27] Perez-Soler R, Chachoua A, Hammond LA, Rowinsky EK, Huberman M, Karp D, Rigas J, Clark GM, Santabarbara P, and Bonomi P (2004). Determinants of tumour response and survival with erlotinib in patients with non–small-cell lung cancer. *J Clin Oncol* **22**, 3238–3247.

[28] Shepherd FA, Rodrigues Pereira J, Ciuleanu T, Tan EH, Hirsh V, Thongprasert S, Campos D, Maoleekoonpiroj S, Smylie M, Martins R, et al. (2005). Erlotinib in previously treated non–small-cell lung cancer. *N Engl J Med* **353**, 123–132.

[29] Giaccone G, Herbst RS, Manegold C, Scagliotti G, Rosell R, Miller V, Natale RB, Schiller JH, Von Pawel J, Pluzanska A, et al. (2004). Gefitinib in combination with gemcitabine and cisplatin in advanced non–small-cell lung cancer: a phase III trial—INTACT 1. *J Clin Oncol* **22**, 777–784.

[30] Herbst RS, Giaccone G, Schiller JH, Natale RB, Miller V, Manegold C, Scagliotti G, Rosell R, Oliff I, Reeves JA, et al. (2004). Gefitinib in combination with paclitaxel and carboplatin in advanced non–small-cell lung cancer: a phase III trial—INTACT 2. *J Clin Oncol* **22**, 785–794.

[31] Herbst RS, Prager D, Hermann R, Fehrenbacher L, Johnson BE, Sandler A, Kris MG, Tran HT, Klein P, Li X, et al. (2005). TRIBUTE: a phase III trial of erlotinib hydrochloride (OSI-774) combined with carboplatin and paclitaxel chemotherapy in advanced non–small-cell lung cancer. *J Clin Oncol* **23**, 5892–5899.

[32] Fung AS and Tannock IF (2007). Potential of gefitinib to inhibit repopulation of tumor cells between courses of paclitaxel: implications for scheduling [abstract]. In *Proceedings of the 98th Annual Meeting of the American Association for Cancer Research; 2007 Apr 14-18; Los Angeles, CA*. American Association for Cancer Research, Philadelphia, PA. Abstract 5422.

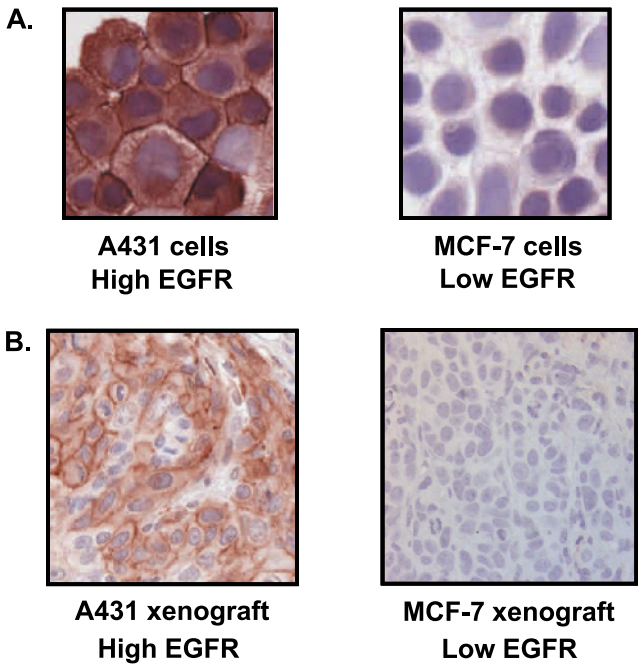

Figure W1. EGFR expression in (A) human squamous cell carcinoma (A431) and human breast cancer (MCF-7) cells and (B) A431 and MCF-7 xenografts.